Journal of Volcanology and Geothermal Research 280 (2014) 53–66

Contents lists available at ScienceDirect

Journal of Volcanology and Geothermal Research

journal homepage: www.elsevier.com/locate/jvolgeores

A newly-emerged (August 2013) artificially-triggered fumarole near the Fiumicino airport, Rome, Italy

Pio Sella [a], Andrea Billi [b,*], Ilaria Mazzini [b,c], Luigi De Filippis [c], Luca Pizzino [d], Alessandra Sciarra [d], Fedora Quattrocchi [d]

[a] Geomagellan, Montecompatri, Rome, Italy
[b] Consiglio Nazionale delle Ricerche, IGAG, Rome, Italy
[c] Dipartimento di Scienze, Università Roma Tre, Rome, Italy
[d] Istituto Nazionale di Geofisica e Vulcanologia, Rome, Italy

ARTICLE INFO

Article history:
Received 20 November 2013
Accepted 6 May 2014
Available online 14 May 2014

Keywords:
Fumarole
Mud volcano
Gas hazard
Drilling
Rome

ABSTRACT

Early in the morning of 24 August, 2013, following by hours the drilling of a shallow borehole in the same spot, a new fumarole producing emissions of CO_2-rich gas, water, and mud suddenly appeared at a crossroad along the fenced area of the Fiumicino international airport of Rome, Italy. Similar episodes have been scientifically documented or simply reported in recent and past years. To understand why gases are easily entrapped in the shallow subsurface of the Fiumicino area, we used five borehole cores drilled by us, analyzed the stratigraphy of these and other nearby cores, acquired a 2D seismic refraction tomogram, and performed chemical and isotopic analyses of water samples collected from aquifers intercepted by two drilled boreholes. Our boreholes were realized with proper anti-gas measures as, while drilling, we recorded the presence of pressurized gases at a specific permeable gravel level. Results show that, in the study area, gases become mainly entrapped in a mid-Pleistocene gravel horizon at about 40–50 m depth. This horizon contains a confined aquifer that stores the endogenous upwelling gases. The gravel is interposed between two silty–clayey units. The lower unit, very hard and overconsolidated, is affected by fractures that allow ascending gases to bypass the otherwise impermeable shale, permeate the gravel, and dissolve into the aquifer. In contrast, the upper unit is impermeable to fluids and seals the gas-pressurized aquifer, which therefore constitutes a source of hazard during human activities such as well drilling, quarrying, and various building-related excavations. As the stratigraphy of the Fiumicino area is very common in large portions of the densely populated Roman area and as the adjacent volcanic districts are hydrothermally active, we conclude that phenomena similar to that observed at Fiumicino could again occur both at Fiumicino and elsewhere in the surrounding region. As a prompt confirmation of our conclusion, we signal that, while writing this paper, new artificially-triggered degassing phenomena occurred off Fiumicino in connection with the construction of the new harbor.

1. Introduction

Suddenly on the early morning of 24 August 2013, a fumarole producing emissions of gas (mainly CO_2), cold water (c. 20 °C), and mud appeared at a crossroad along the fenced area of the Fiumicino international airport of Rome, Italy (Figs. 1 and 2; Supplemental Materials 1 to 3; Ciotoli et al., 2013; Pantaloni and Argentieri, 2013). For weeks the fumarole has continued its emissions, forming, at times, a small mud volcano (Fig. 2). The emissions have then slightly decreased and are still active at the time of writing (November 2013). Similar structures are well known as volcanic or endogenous manifestations worldwide including Iceland, Italy, Japan, and Yellowstone and Salton Sea in the USA, and are potentially hazardous when occurring in or close to inhabited areas both for the emitted lethal gases and for other connected phenomena such as mudflows (Werner et al., 2000; Hannington et al., 2001; Kopf, 2002; Patrick et al., 2004; Manga and Brodsky, 2006; Barberi et al., 2007; Caliro et al., 2007; Etiope et al., 2007; Giammanco et al., 2007; Ohba et al., 2007; Mazzini, 2009; Chiodini et al., 2012).

The city of Rome is located in the Tyrrhenian (western) side of the central Italian peninsula (Fig. 1). This area constitutes the rear of the Cenozoic–Quaternary east-verging Apennines fold-and-thrust belt and has been stretched by backarc and postorogenic processes since middle Miocene time (Brogi and Liotta, 2008; Barchi, 2010; Brogi, 2011). In this region, a shallow Moho (Fig. 1a), Quaternary extensional basins and volcanoes, and high heat and deep CO_2 fluxes are the main symptoms of the Quaternary-to-present stretching processes (Peccerillo, 1985; Malinverno and Ryan, 1986; Sartori and ODP LEG 107 Scientific Staff, 1989; Mongelli and Zito, 1991; Faccenna et al., 1994a; Cavinato and

* Corresponding author at: CNR-IGAG at Dipartimento Scienze della Terra, Università Sapienza, Piazzale A. Moro 5, Rome 00185, Italy. Tel.: +39 06 4991 4955.
E-mail address: andrea.billi@cnr.it (A. Billi).

http://dx.doi.org/10.1016/j.jvolgeores.2014.05.008
0377-0273/

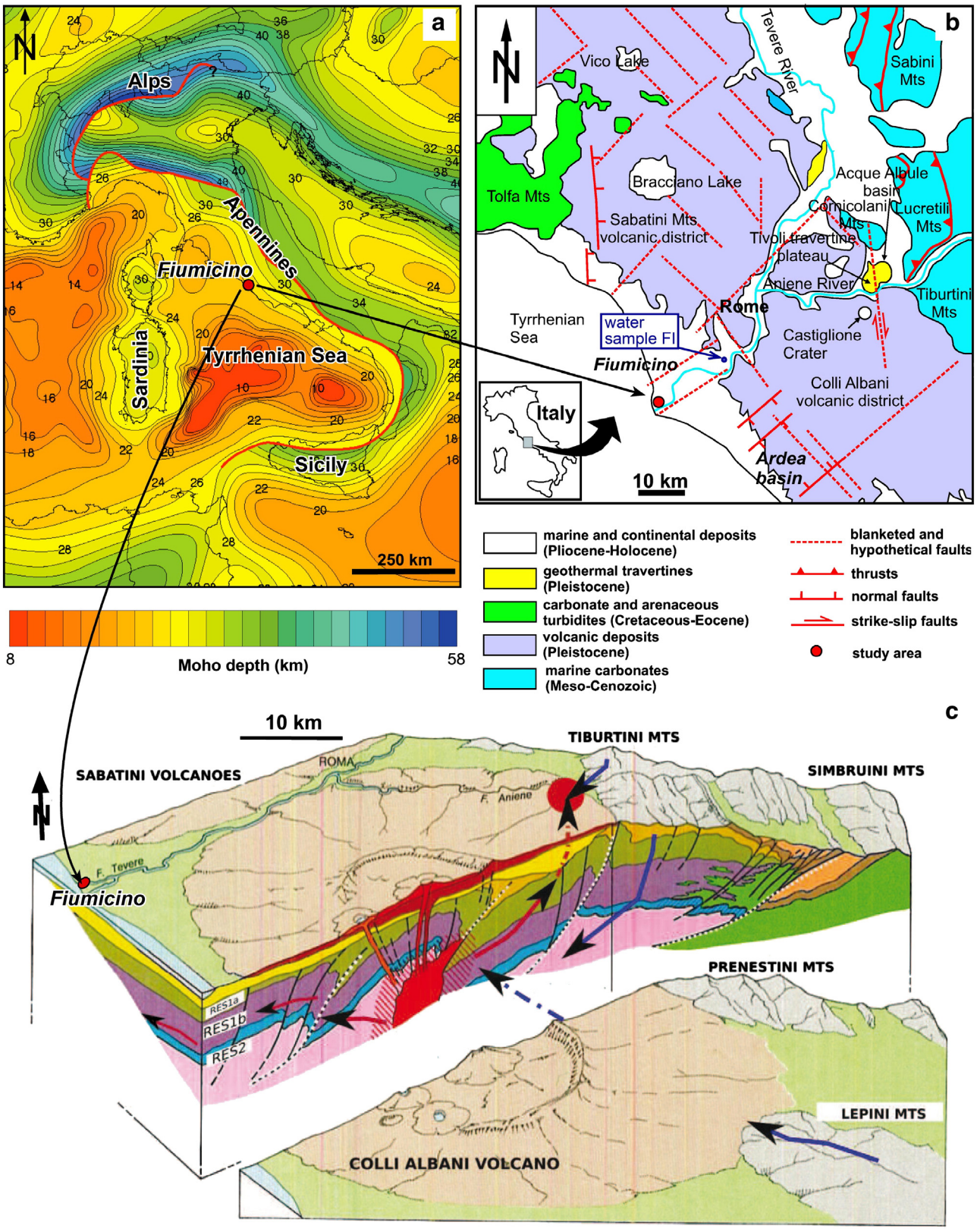

Fig. 1. (a) Depth to the Mohorovičić discontinuity (Moho) in Italy and surrounding areas (after Dèzes and Ziegler, 2002). Numbers in the map are Moho depth in kilometers. The crust of the Tyrrhenian (western) side of the Italian peninsula (where Fiumicino is located) has been stretched and thinned by postorogenic processes. The Tyrrhenian basin is where the thinnest crust of western Europe–Mediterranean occurs. (b) Geological setting of the Roman area dominated by the Tiber River valley (Roman basin) and two adjacent large volcanic districts of Quaternary age: the Sabatini district toward the northwest and the Colli Albani district toward the southeast. The study area (Fiumicino) is located on the Tiber River delta along the Tyrrhenian coast. (c) Three-dimensional diagram showing the Colli Albani subsurface geological structure (after De Rita et al., 1988, modified by Giordano et al., 2013). See the Fiumicino area located on the Tiber River delta.

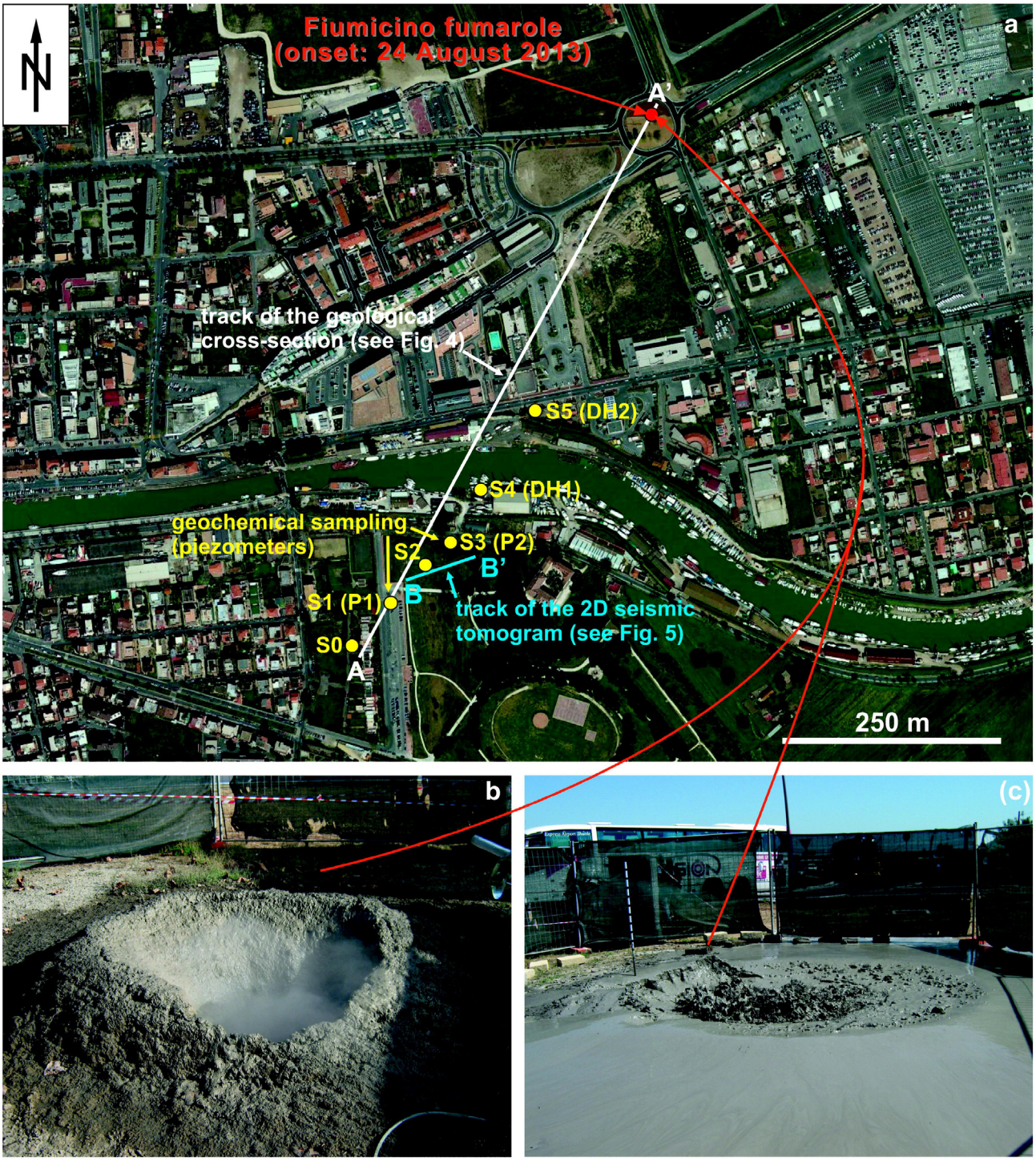

Fig. 2. (a) Location map (from Bing Maps) showing: (red) the Fiumicino fumarole (Latitude: 41°46′32.43″N; Longitude: 12°14′26.57″E); (yellow) the stratigraphic boreholes studied in this paper (Figs. 3 and 4); (white) the track of the geological cross-section shown in Fig. 4; (blue) the track of the 2D seismic tomogram shown in Fig. 5; and (yellow) the geochemical sampling sites (see related results in Figs. 6–8). The location of the water sample FI is shown in Fig. 1(b) (Table 1). (b) Photograph of the Fiumicino fumarole at the onset of its activity with the emission of mostly gases. (c) Photograph of the Fiumicino fumarole during its successive activity with the emission of gases, mud, and water. (For interpretation of the references to color in this figure, the reader is referred to the web version of this article.)

DeCelles, 1999; Chiodini et al., 2000; Gambardella et al., 2004; Acocella and Funiciello, 2006; Billi et al., 2006; Billi and Tiberti, 2009; Brogi and Capezzuoli, 2009; Brogi et al., 2010; Giordano et al., 2013). The city of Rome, in particular, has been built along the Tiber River valley between two Quaternary large volcanic districts: the Colli Albani district toward the southeast and the Sabatini district toward the northwest (Funiciello and Parotto, 1978; Funiciello, 1995; Alvarez et al., 1996; Bozzano et al., 2008; Funiciello et al., 2008; Funiciello and Giordano, 2010; Milli et al., 2013). This latter volcanic district started its activity around 600 ka and has been vigorously active until at least late Pleistocene time (Funiciello et al., 1976; Cioni et al., 1993; De Rita et al., 1996; Sottili et al., 2010; Sottili et al., 2012). The activity of the Colli Albani volcano, which is very close to (partly beneath) Rome, started around 700–600 ka and its most recent hydrothermal activity (late Pleistocene to present time) has influenced the life, urbanization, and development of Rome since its birth in the 1st Millennium B.C. (De Rita et al., 1988;

Karner et al., 2001; Giordano et al., 2006; Marra et al., 2009; Funiciello and Giordano, 2010; Gioia et al., 2010). At present, the Colli Albani volcano is classified as quiescent for its numerous recent and historical hydrothermal manifestations including a few episodes, during Holocene and historical times, of maar lake withdrawals with convective rollover of the lake water down over the caldera flank toward the actual city of Rome (Funiciello et al., 2002, 2003; Giordano et al., 2002; Giaccio et al., 2007; De Benedetti et al., 2008).

Active hydrothermal springs and related deposits are numerous all over the large Roman area (Barbieri et al., 1979; Maiorani et al., 1992; Minissale et al., 1997; Quattrocchi and Calcara, 1998; Chiodini and Frondini, 2001; Minissale et al., 2002; Billi et al., 2007; Voltaggio and Spadoni, 2007; Chiodini et al., 2008; Faccenna et al., 2008; Cinti et al., 2011; De Filippis et al., 2013a,b; Quattrocchi et al., 2013). Gas, steam, and fire emission, rumbling, noises, increase of water temperature, and several other hydrological and hydrothermal manifestations have been documented by historical sources for the Colli Albani volcano during historical times (Funiciello et al., 2002, 2003; Tuccimei et al., 2006). In the last years, accidental gas blowouts have occurred during shallow well drillings in the western sector of the volcano and also in the Fiumicino area (Barberi et al., 2007), showing the presence of gas pressurized aquifers confined under shallow impermeable horizons (Chiodini and Frondini, 2001; Pizzino et al., 2002; Annunziatellis et al., 2003; Beaubien et al., 2003; Carapezza and Tarchini, 2007; Carapezza et al., 2012). These manifestations are potentially dangerous for the emissions of lethal gases including H_2S and CO_2, this latter gas being always one of the fundamental components of these emissions (Gambardella et al., 2004). It follows that understanding the subsurface geological setting where these manifestations occur is the prerequisite to know the cause and mechanism of gas manifestations and, ultimately, to prevent these manifestations or at least to attenuate their consequences. Of particular relevance is to understand the geological reasons that lead endogenous gases to accumulate in the shallow subsurface, where these gases constitute a source of hazard during human activities such as well drilling, quarrying, and various building-related excavations (e.g., Barberi et al., 2007).

At the time of the Fiumicino fumarole first emergence (24 August, 2013), one of us (P.S.) was conducting a stratigraphic and geophysical campaign in an area close to the fumarole (Fig. 2). Below, we present these data to contribute to the understanding of the geological-stratigraphic setting in which the newly emerged fumarole has occurred. We have also sampled the shallow aquifers from two drilled wells in the study area to determine the origin of both waters and dissolved carbon (i.e., CO_2). These latter data have been compared with C-isotopes from the CO_2 emitted by the fumarole (Ciotoli et al., 2013). All these multidisciplinary data contribute to the understanding of the fumarole development and may constitute the geological database for future advanced studies on the Fiumicino fumarole and other similar phenomena nearby. As we know that the fumarole was artificially-triggered by borehole drilling (see details in the discussion section), we aim, in particular, at comprehending how and why the gas was entrapped before its sudden release caused by man-related activities.

2. Geological setting

The Fiumicino fumarole is located about 20–25 km to the west-southwest of the Rome city center, in the area of the Tiber River delta along the Tyrrhenian coast (Figs. 1 and 2). The Roman basin, which includes most part of the city of Rome and also the Fiumicino study area, developed since late Pliocene time and was accompanied by a continuous regional tectonic uplift (Milli, 1997; Bordoni and Valensise, 1998; Giordano et al., 2003; Milli et al., 2013) and by an intense volcanic activity with a climax in middle–late Pleistocene time when the near volcanic districts developed (Locardi et al., 1976; Cioni et al., 1993; De Rita et al., 1993, 1995; Karner et al., 2001). The Monte delle Piche Formation (MDP) locally forms the hardground basement of the Roman basin (Milli et al., 2013). This formation consists of overconsolidated gray silty clays, interbedded with sand levels. Due to its brittle behavior connected with the overconsolidation state, the formation is, in places, characterized by fractures (Funiciello and Giordano, 2008; Giordano and Mazza, 2010). Toward the west, the hard clayey deposits of the MDP pass with tectonic contact to the clays of the Lower Pliocene Marne Vaticane Formation (MVA; Funiciello and Giordano, 2008). Those clayey deposits are known all over the Roman basin at various elevations mostly from borehole logs but also from outcrops. The elevation variations are mainly due to Pleistocene extensional faults that controlled and dismembered the Roman basin (Funiciello et al., 1976, 2008; Funiciello and Parotto, 1978; Faccenna et al., 1994b; Di Filippo and Toro, 1995; Funiciello, 1995; Giordano et al., 2003). Recently, the stratigraphy of the Tiber River delta area has been studied in detail through several sediment cores (Marra et al., 2013; Milli et al., 2013). Through these investigations, the Monte delle Piche Formation (MDP; Lower Pleistocene) and the Ponte Galeria Sequence (PGS; Late Lower Pleistocene–Holocene) have been identified. The two sequences are separated by a polygenic erosional surface that formed during the sea-level fall between MIS31 and MIS27 (Milli et al., 2013). In particular, above a gravel layer that can be considered a marker of the PGS succession, a complex deposit of silts, clays, and sands constitutes the Tiber Depositional Sequence (TDS), showing the transformation of the Tiber delta from a wave dominated estuary to a wave dominated delta with increasing river power (Milli et al., 2013). The main target of this paper is the above-mentioned gravel layer, which, at least in the study area (Fiumicino), hosts a gas pressurized confined aquifer.

The fumarolic phenomenon occurred since August 2013 in the Fiumicino area (Ciotoli et al., 2013) is not at all an extraordinary event (Pantaloni and Argentieri, 2013). In 2005, in a locality close to the fumarole studied in this paper (Fiumicino), a borehole drilled down to about 27 m depth caused a sudden gas blowout with emission of CO_2 accompanied by minor discharge of N_2 and CH_4 (Barberi et al., 2007). These same authors mentioned at least three previous similar events occurred in the same area (Fiumicino) within a few past years. Moreover, in May 1925, in a site 400 m distant from the fumarole emerged in August 2013, while constructing a glass factory, the drilling of a borehole down to 40 m depth triggered the emergence of a fumarole with emission of water, mud, gravel, and gases. As the emission did not cease soon, the borehole was plugged after only a few days, but minor emissions kept existing for about one year in the surrounding construction area where drilling and excavations were active (Novarese, 1926; Argentieri and Pantaloni, 2013; Pantaloni and Argentieri, 2013). Novarese (1926) reported also similar events that occurred in the Roman area prior than 1925. Of particular interest is the gaseous eruption triggered in 1890 by the drilling of a borehole in the area of the Ostia dewatering plant located along the Tyrrhenian coast circa 5 km to the southeast of Fiumicino. The eruption, with emission of gas, water, and mud, occurred when the borehole reached the depth of 128 m. A further eruption occurred when the borehole reached the depth of 194 m (Novarese, 1926; Pantaloni and Argentieri, 2013).

3. Methods and results

3.1. Stratigraphy

Stratigraphic results from five boreholes (S1, S2, S3, S4, and S5) drilled by one of us (P.S.) in the Fiumicino area are shown in Figs. 3 and 4. Fig. 4 combines our results with those from a previously drilled borehole (S0). The boreholes reached a maximum depth of about 70 m intercepting various continental and marine sediments. For the aims of this paper, in addition to the micropaleontological analyses depicted below (Fig. 3), it is important to mention information from the analyzed boreholes and cores: (1) as observed during drilling, the gravel layer located at about 40–50 m depth (Fig. 4) hosts a confined gas pressurized aquifer such that proper anti-gas measures had to be

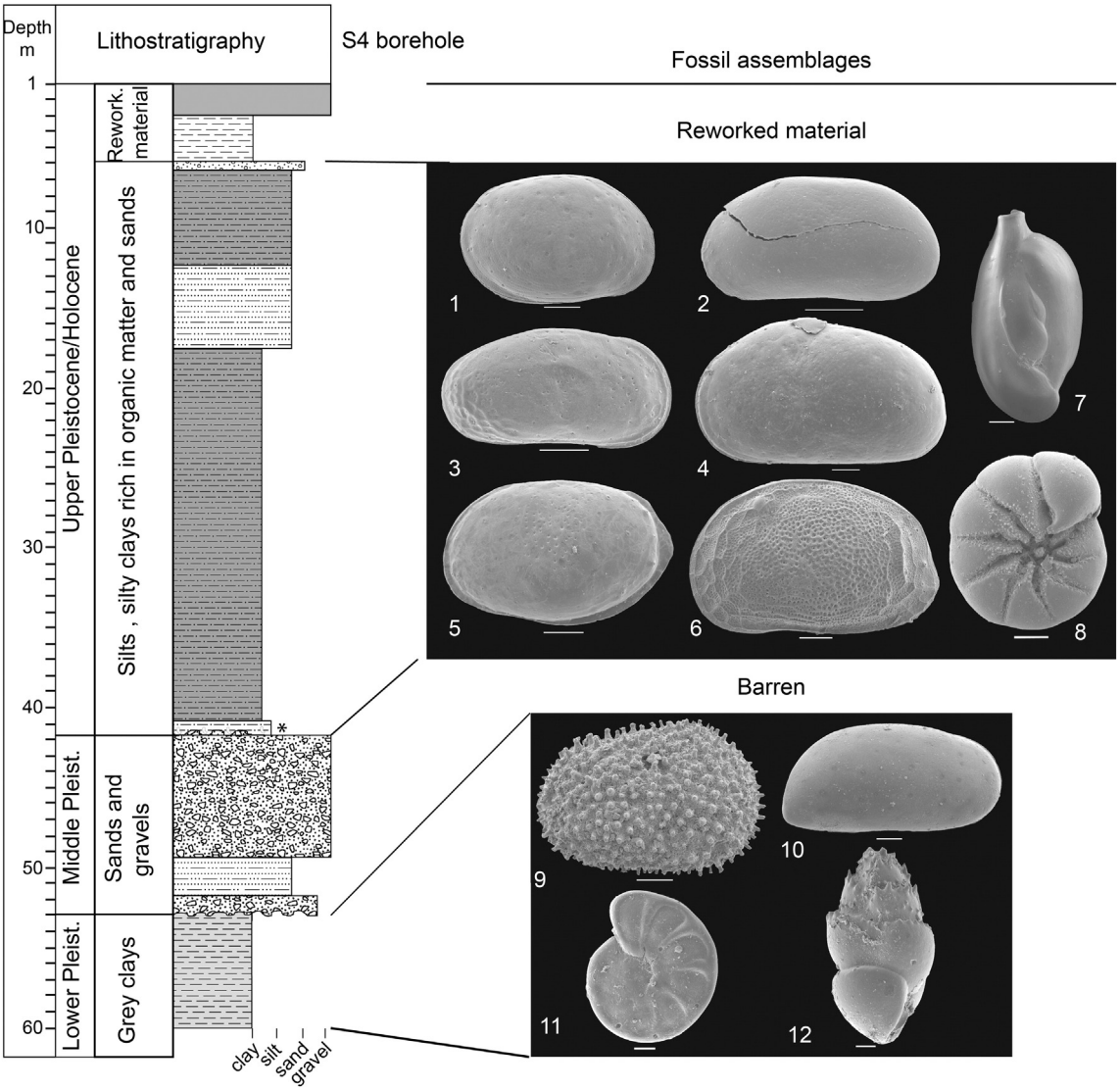

Fig. 3. Stratigraphic log of the S4 sediment core (see location in Fig. 2). Lithostratigraphy and fossil content are shown. 1) *Loxoconcha stellifera*; 2) *Pseudocandona marchica*; 3) *Leptocythere ramosa*; 4) *Cyprideis torosa*; 5) *Palmoconcha turbida*; 6) *Hemicytherura deflorei*; 7) *Triloculina schreiberiana*; 8) *Ammonia parkinsoniana*; 9) *Henryhowella partenopea*; 10) *Krithe exigua*; 11) *Bulimina marginata*; 12) *Hyalinea baltica*. Scale bars = 100 μ. The asterisk on the right of the log indicates the layer rich in carbonate micro-concretions. Core photographs are shown in Fig. S1.

taken during drilling (i.e., S4 and S5 boreholes); (2) a shallower unconfined aquifer is hosted in the sands lying at about 10 m depth and in the upper sediments (i.e., S1 to S5 boreholes; Fig. 4); and (3) carbonate micro-concretions filling the available pores were observed in the clayey silts topping the gravel layer at about 45 m depth (i.e., S4 and S5 boreholes; Fig. 3).

The micropaleontological analyses were performed on about 20 samples from the S4 sediment core (Fig. 3). The lowermost stratigraphic unit consists of clay and silty clay with sandy levels. The foraminiferal assemblage is characterized by typical circalittoral benthonic taxa (*Bolivina* spp., *Bulimina* spp., *Hyalinea balthica*, *Cibicidoides pachyderma*, *Textularia*) and significant frequencies of planktonic species (*G. bulloides*, *G. ruber*, *Glorotalia inflata*, *Neogloboquadrina pachyderma and Turborotalia quinqueloba*). The ostracod assemblage is characterized by *Henryhowella partenopea*, *Krithe exigua*, and *Cytheretta* spp. Such assemblage suggests an offshore environment and an age attribution to the Lower Pleistocene (Emilian) for the occurrence of *H. baltica*.

Through a sharp lithological change, the sequence passes to gravels and sandy gravels. The pebbles are mainly derived from carbonate rocks of the Apennines. Such deposits do not contain any fossils. They have been attributed to fluvial and beach environments of the Ponte Galeria Formation (Middle Pleistocene, Bellotti et al., 1995).

Another dramatic lithological change marks the passage to the silts and silty clays with sandy layers. The foraminiferal assemblage is characterized by benthonic taxa typical of shallow waters rich in organic matter (*Ammonia parkinsoniana*, *Triloculina schreiberiana*, *Adelosina* spp.). The ostracod assemblage is typical of coastal lagoons and estuaries with strong freshwater inputs linked to the nearby river (*Cyprideis torosa*, *Pseudocandona marchica*, *Pontocythere turbida*, *Palmoconcha turbida*, *Loxoconcha stellifera*, *Candona* spp. *Ilyocypris* spp.). These associations are typical of the Tiber Depositional Sequence, attributed to the Upper Pleistocene–Holocene.

From the visual inspection of the other borehole cores (S0, S1, S2, S3, and S5), we inferred a stratigraphy very similar to the one of the S4 core (Fig. 3), at least for the middle and deepest portions (Fig. 4). The S4 and S5 cores differ from the other four cores only for the shallowest 5–6 m, where (S4 and S5) reworked recent material occurs along the partly-artificial banks of the Fiumicino Channel. Hence, in Fig. 4, we propose a cross-sectional stratigraphic correlation among the six boreholes. This correlation is substantially consistent with previous borehole-

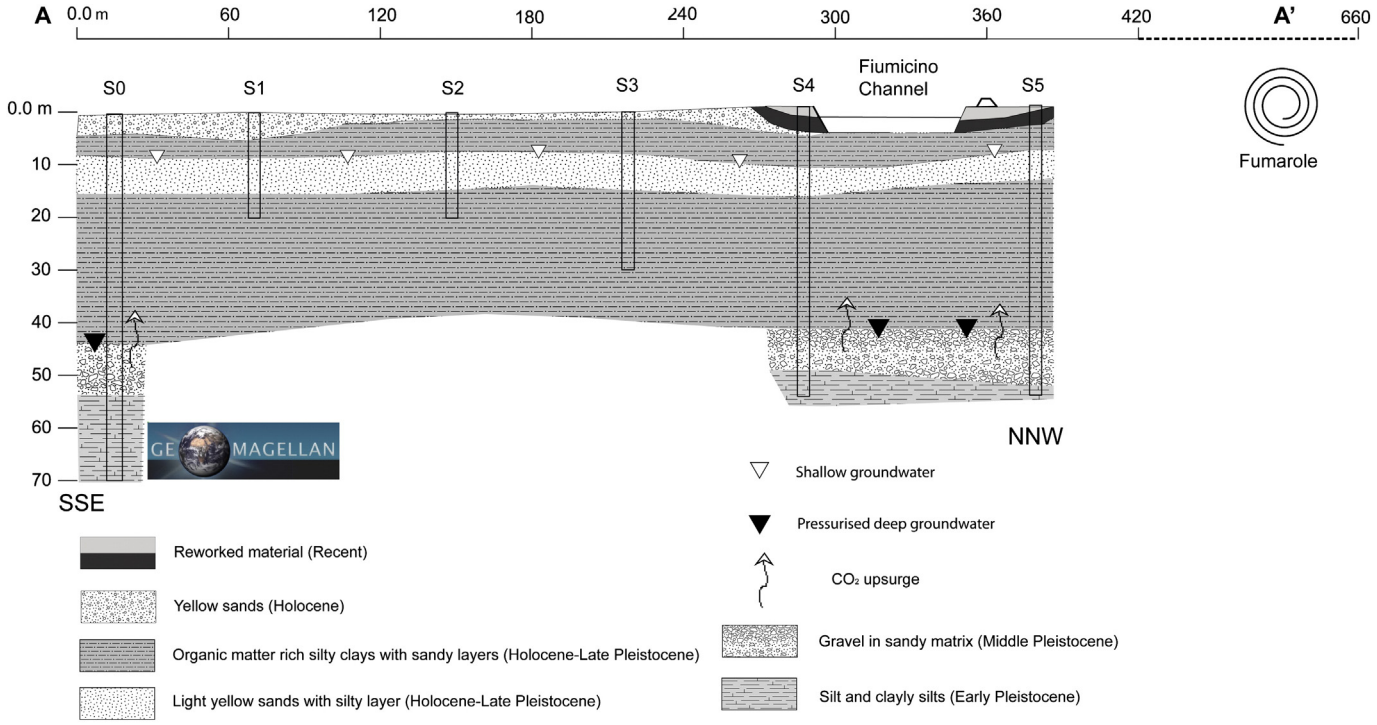

Fig. 4. Geological cross-section through the study area (see track in Fig. 2a). The cross-section is based on the S0 to S5 borehole cores whose stratigraphy is shown along the cross-section. The presence of confined and unconfined aquifers as recorded during drilling is also shown with filled and unfilled triangles, respectively.

core-based stratigraphic models in the same or nearby areas (e.g., Bellotti et al., 1995; Bozzano et al., 2008; Funiciello and Giordano, 2008; Funiciello et al., 2008; Praturlon, 2008; Raspa et al., 2008; Marra et al., 2013; Milli et al., 2013).

3.2. Geophysics

To understand the subsurface setting of the Fiumicino area and, in particular, the lateral continuity vs. variability of the stratigraphic succession observed in the borehole cores (Fig. 4), we completed a 2D seismic refraction tomogram (e.g., Bais et al., 2003; Heincke et al., 2010) across the study area. The tomogram is shown in Fig. 5 whereas its track is shown in Fig. 2(a). We used 24 geophones placed along the profile with a spread length of 5 m. This setting was chosen to obtain good ray coverage at depths down to 60 m at least. As energy sources, we used explosives with charges of 27 g placed in 30–40 cm deep well. Data collection was performed with five 24-channel recording units with a spread length of 24 m. Data were then inverted using a smoothness constrained minimization algorithm in the RAYFRACT software to obtain the tomogram of Fig. 5. The profile is stratigraphically calibrated using results from the near S4 borehole (Figs. 2a, 4, and 5).

The most evident feature of the tomogram shown in Fig. 5 is the approximately flat attitude of the P-wave velocity (Vp) domains, indicating a general flat geometry of the investigated stratigraphy. The tomogram shows a general increase of the P-wave velocity (Vp) with depth from a minimum of 100–200 m/s to a maximum of about 1000 m/s at a depth of about 60–70 m. A horizontal pattern of curves separating different Vp domains is observed, particularly at depths greater than 35 m. Above 35 m, the velocity pattern is more irregular and the velocity gradient with depth is low (c. 100 m/s every 10 m), probably due to the presence of loose shallow material. Below 35 m of depth, this gradient increases becoming about 100 m/s every 5 m

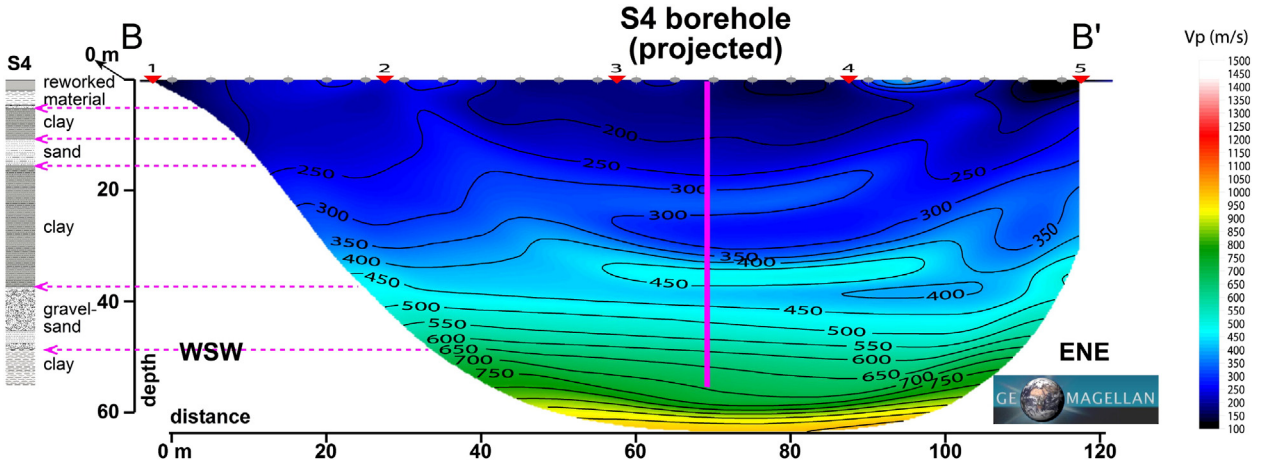

Fig. 5. 2D tomographic velocity model obtained from the seismic refraction profile whose track is shown in Fig. 2(a). The tomogram has been calibrated using the stratigraphy of the S4 borehole (Fig. 4) that has been projected on the center of the tomogram. A synthetic stratigraphy of the S4 borehole is shown on the left side of the figure.

depth and the curves become almost flat probably because of the presence of compact horizontal deposits (clay, sandy clay, and gravel). Below the gravel (below 55–60 m of depth), the velocity gradient doubles again becoming circa 100 m/s every 2–3 m depth in coincidence with the occurrence of very compact horizontal clays (compare Figs. 4 and 5).

3.3. Water geochemistry

Chemical and isotopic measurements in groundwater were performed in piezometers S1 (P1) and S3 (P2), collecting water at a depth of −15.30 and −24.30 m, respectively. In addition to these groundwater samples, for comparison, chemical data from both an 18 m deep well (FI) located in the inner sector of the study area (see location in Fig. 1b), and from local seawater (SW, Cinti et al., 2011), are reported. The main aim of the geochemical analysis was to determine the origin of the circulating fluids, with specific focus to the provenance of the dissolved carbon, assessing its relationship with the stratigraphic setting of the area.

Water temperature, pH, redox potential (Eh), and electrical conductivity (salinity) were determined in situ with portable instruments previously calibrated with standard solutions. Alkalinity was measured on the field through titration with 0.05 N HCl and methyl-orange as indicator. Water samples were filtered (0.45 μm) and stored in high-density polyethylene flacons for laboratory analysis. Major anions (Cl^-, Br^-, SO_4^{2-} and NO_3^-) and cations (Ca, Mg, Na and K) were analyzed by ion-chromatography (Dionex, DX500) on filtered and on filtered and acidified samples, respectively. The analytical error for major elements was <10%. The total dissolved carbon (TDIC, representing the sum of the concentrations of the inorganic carbon species in solution, i.e., $CO_{2\ (aq)}$, HCO_3^-, and CO_3^{2-}) was computed by using the PHREEQC code v. 2.12 (Parkhurst and Appelo, 1999), operating with the Lawrence Livermore National Laboratory (LLNL) database, having as input temperature, pH, Eh, alkalinity, and major elements. The carbon isotopic ratios of TDIC, expressed as $\delta^{13}C$ ‰ vs. VPDB, were analyzed by mass spectrometry (Finnigan Delta Plus) following the procedure described by McCrea (1950).

Waters from piezometers P1 and P2 show a very high salinity (TDS ranging from 21,826 to 29176 mg/l), quasi neutral pH, and alkalinity spanning from 15.60 to 27.10 mmol/l. Sample FI shows medium salinity (TDS = 1115 mg/l), slightly acidic pH, and 11.3 mmol/l of alkalinity.

Inspection of the classical Ludwig–Langelier diagram (Fig. 6a), based on the relative amounts of major ions, along with Ca–Mg–Na and Cl–SO_4–HCO_3 ternary plots (Fig. 6b and c) allow us to put forward some general hypotheses on the origin of the sampled waters. A first look at Fig. 6a, b, and c points out a great difference in the chemical compositions of samples P1 and P2 with respect to sample FI. Waters from piezometers stand in the chloride-alkaline field, close to the point representative of the local seawater composition, while sample FI falls in the field of the freshwaters, having a bicarbonate-earth chemistry. Sample FI was taken as representative of the waters circulating in the inner Fiumicino territory, not affected by seawater contamination (see explanations below). Therefore, despite of its saline content (TDS = 1115 mg/l), FI will be considered as the freshwater term in the reported binary and ternary plots (Figs. 6 and 7).

To understand the relationships between Na–Cl samples and both local seawater and freshwaters, chemical characteristics of these two "end-members", mainly referred to their major element composition and ion ratios, have to be considered. Seawater in general has a uniform chemistry due to a long residence time of major constituents with the predominance of Cl and Na, showing a molar ratio of 0.86 (0.84 for the local Tyrrhenian seawater, Cinti et al., 2011). Seawater solutes are specifically characterized by an excess of Cl over the alkali ions (Na and K) and Mg greatly in excess of Ca and anions ($SO_4 + HCO_3$). In contrast, continental fresh groundwater is characterized by highly variable chemical compositions, although the predominant anions are HCO_3 with minor amounts of SO_4 and Cl. If not anthropogenically polluted, the fundamental cations are Ca and Mg and, to a lesser extent, the alkali ions Na and K. In most cases Ca predominates over Mg.

Fig. 6a–c shows that samples P1 and P2 are positioned next to the theoretical line between freshwater (FI) and local seawater (SW), slightly deviating from this line due to their remarkable bicarbonate enrichment (see below). FI sample is characterized by the following ionic abundance: Ca > HCO_3 > SO_4 > Mg > Cl > Na > K, typical, at least for Ca and HCO_3, of waters in the early stage of interaction between meteoric waters and rocks (including soils). SO_4 and Cl contents could stem from slightly saline fluids trapped into the shallow sediments cropping out in the area (Capelli et al., 2008). The presence of both sulfate and chlorine fully justifies the position of FI toward the Ca–SO_4 (Cl) quadrant (Fig. 6a).

Besides the major chemical compositions, the geochemical state of the boreholes was assessed by displaying the ionic ratio analysis, including Na/Cl, Br/Cl, and HCO_3/Cl (Fig. 7a–c). Cl is generally taken as a conservative non-reactive element. Once added to the solution, it remains unaltered and is not removed by any chemical processes such as precipitation, adsorption on mineral surfaces, cation exchange, or redox reactions. Here we hypothesize that Cl comes from seawater only, being representative of marine contribute in non-saline aquifers.

The Na vs. Cl binary diagram (Fig. 7a) evidences that all samples lie on the theoretical line between freshwater (FI) and local seawater (SW), suggesting that the relatively high concentrations of Na and Cl may be ascribed to a progressive fluid contribution from seawater. Also the Br/Cl ratio (Fig. 7b) strongly supports the interaction of the sampled waters with salty fluids of marine origin.

The observed Na–Cl chemistry and ion ratios so far presented could be related to a well known phenomenon that is currently going on in the study area. The Fiumicino coastal sector (Tiber River delta), in fact, as many other coastal sectors in Italy, is experiencing widespread saltwater contamination of water supply wells. This problem, in particular, has emerged in the last ten years (Barrocu, 2003; De Luca et al., 2004; Capelli and Mazza, 2008). Increased and uncontrolled groundwater pumping over time is the primary cause of saltwater intrusion. As a consequence, the contaminated water progressively undergoes a quality deterioration (Total Dissolved Solids > 20 g/l), eventually resulting unfit both for domestic and for agricultural purposes. The saline wedge (8 m thick, with TDS = 35 g/l) has been detected at a depth of 13 m in the waters of the Fiumicino Channel (Capelli and Mazza, 2008), very close to the P1 and P2 sites (Figs. 2 and 4). Moreover, in a piezometer located a few kilometers to the south of Fiumicino, highly saline water (TDS = 23 g/l, Capelli and Mazza, 2008) has been found at a depth of 25.9 m, confirming that seawater intrusion in the study area is widespread. This process seems unrelated with the distance from the shoreline, rather with the depth of the wells (De Luca et al., 2004). The subsurface seawater encroachment is less evident toward the inner part of the Fiumicino area (i.e., toward Rome; Capelli et al., 2008), where groundwater is unaffected by saline contamination (e.g., FI site).

The values of HCO_3 vs. Cl (Fig. 7c) are indicative of freshwater contribute and point out a very large difference in the alkalinity content of the sampled groundwater with respect to seawater. Generally, in case of seawater intrusion, the HCO_3/Cl ratios gradually decrease and approach the seawater value as Cl (or TDS) increases; consequently, the considered ratio can be considered as a good indicator for salinization due to the seawater encroachment. On the contrary, samples P1, P2, and FI depict a different trend from that individuated by the freshwater–seawater line, due to their higher bicarbonate contents. As a consequence, Fig. 7c implies, for groundwater, an additional carbon source than seawater. To examine the provenance of this external source of carbon, we performed analysis of the $\delta^{13}C_{TDIC}$, whose values range from −19.30 (sample FI) to −11.43‰ (sample P2) vs. VPDB (Table 1). To investigate the various possible sources of the dissolved CO_2, we calculated the pristine carbon isotopic composition of carbon

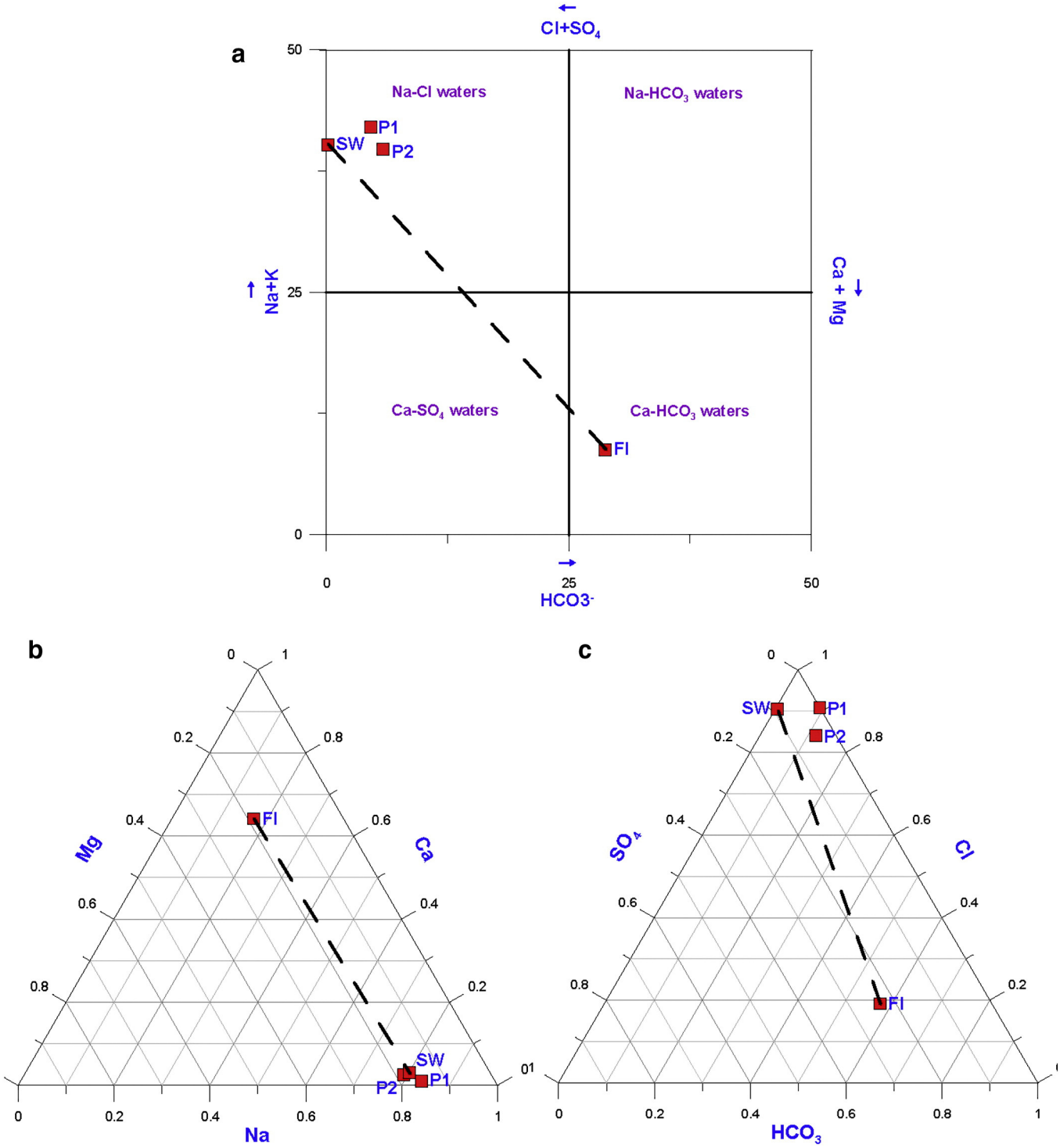

Fig. 6. (a) Ludwig–Langelier diagram, (b) ternary plots of cations, (c) and anions for waters sampled in the Fiumicino area. Dashed line represents the mixing line between the freshwater (FI, see text) and local seawater (SW) end-member.

dioxide interacting with groundwater from the measured $\delta^{13}C$ values of TDIC, using the following equation (Zhang et al., 1995):

$$\delta^{13}C\ CO_{2(gas)} = \delta^{13}C(TDIC) - \left[\left(\varepsilon_{H2CO3-CO2} * \left[CO_{2(aq)}\right]/TDIC\right) + (\varepsilon_{HCO3^--CO2} * [HCO_3^-]/TDIC)\right] + \left(\varepsilon_{CO3^{2-}-CO2} * \left[CO_3^{2-}\right]/TDIC\right)\right]. \quad (1)$$

Eq. (1) takes into account the equilibrium molar ratio of aqueous carbon species at sampling temperature and pH and the isotope enrichment factors (ε) between carbon species and gaseous CO_2 at the same conditions.

As reported in Table 1, the $\delta^{13}C_{CO2}$ computed values are comprised between −25.73‰ (sample FI) and −18.69‰ (sample P2) vs. VPDB. The observed range clearly suggests that dissolved CO_2 in the waters of Fiumicino comes from an organic source, as highlighted in Fig. 8,

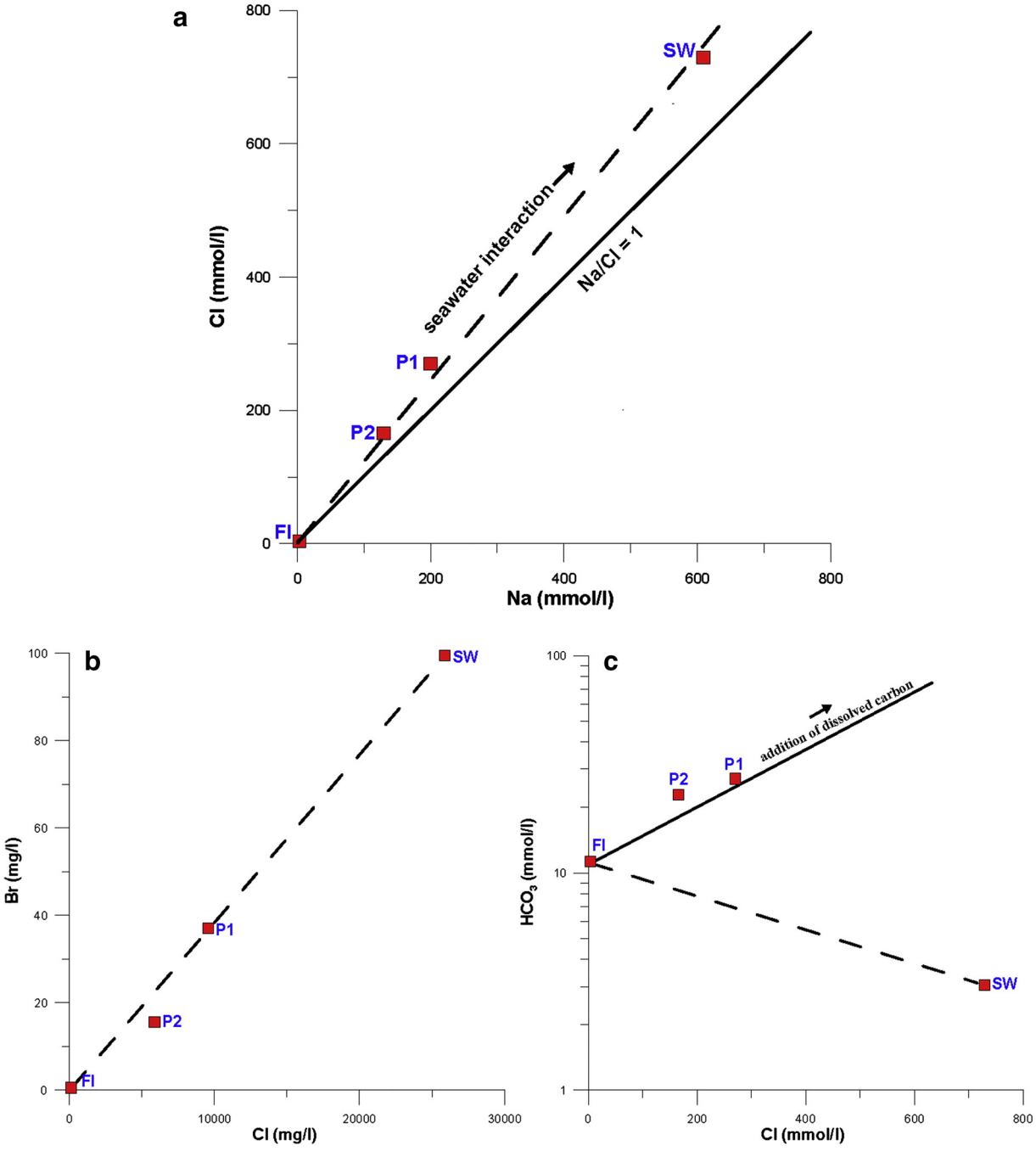

Fig. 7. (a) Na/Cl, (b) Br/Cl, and (c) HCO_3/Cl plots for waters sampled in the Fiumicino area. Dashed line represents the mixing line between the freshwater (FI, see text) and local seawater (SW) end-member. Solid line in plot (c) clearly evidences the position of the P1, P2, and FI samples. They lie far above the freshwater–seawater line, due to their higher bicarbonate contents. As a consequence, for these ground waters, an additional carbon source than seawater is requested.

where total carbon content is plotted vs. calculated $\delta^{13}C_{CO2}$. Negative $\delta^{13}C_{CO2}$ values (−25.73, −23.61 and −18.69‰ vs. VPDB in samples FI, P1, and P2, respectively) in these waters imply dominant CO_2 shallow contribution from plant-root respiration and aerobic decay of organic matter (Cerling et al., 1991). Conversely, the heavier carbon isotope signature in the CO_2-rich gas phase of the fumarole ($\delta^{13}C_{CO2} = -1.0$ and −1.1‰ vs. VPDB, Ciotoli et al., 2013) points to a completely different origin of carbon dioxide, certainly of deep provenance. If we report these data in Fig. 8 (green diamond), CO_2 source(s) could be individuated both in the mantle degassing ($\delta^{13}C_{CO2}$ values from −7.0 to −3.0‰ vs. VPDB; Javoy et al., 1982; Rollinson, 1993) and in the thermo-metamorphic reactions involving carbonate formations ($\delta^{13}C$ of the Apenninic carbonates = 2.2 ± 0.66 vs. VPDB; Chiodini et al., 2004), mixed at various extent, as already claimed by numerous authors for gas vents located in the Tyrrhenian sector of central Italy (Minissale et al., 1997; Chiodini and Frondini, 2001; Minissale, 2004; Mariucci et al., 2008; Cinti et al., 2011; Carapezza et al., 2012), including the Fiumicino area (Barberi et al., 2007). Isotopic values of carbon in the Fiumicino fumarole are in the range of $\delta^{13}C_{CO2}$ values for gas emitted from the Colli Albani and Sabatini volcanoes (Barberi et al., 2007; Mariucci et al., 2008; Cinti et al., 2011), strongly supporting the deep provenance of the gas emitted from the fumarole. Moreover, a similar ^{13}C enrichment (and the same deep origin) was also observed in the CO_2 emitted from shallow boreholes drilled in the Fiumicino area

Table 1
Physico-chemical, chemical, and isotopic data for the waters sampled in the Fiumicino area. Keys: n.d. = not determined.

Sample	Latitude	Longitude	T (°C)	pH	Eh (mV)	El. Cond. (μS/cm) at 25 °C	TDS (mg/l)	Cl^- (mmol/l)	Br^- (mg/l)	NO_3^- (mg/l)	SO_4^{2-} (mmol/l)	HCO_3^- (mmol/l)	Na^+ (mmol/l)	K^+ (mmol/l)	Mg^{2+} (mmol/l)	Ca^{2+} (mmol/l)	Total carbon (mmol/Kg)	$\delta^{13}C_{TDIC}$ (meas.) ‰ vs. VPDB	$\delta^{13}C_{CO2}$ (calc.) ‰ vs. VPDB
P1	41.7700	12.2368	20.5	7.20	−49	31,180	21,826	270.00	37.0	4.59	0.29	27.10	199.87	5.63	36.68	2.36	36.30	−16.06	−23.61
P2	41.7708	12.2375	18.5	7.02	−10	41,680	29,176	165.77	15.6	4.27	8.39	22.90	129.71	3.27	30.10	4.21	32.27	−11.43	−18.69
FI	41.8142	12.3890	18.2	6.90	50	1593	1115	3.76	0.5	n.d.	4.60	11.30	3.51	0.15	3.91	13.29	17.31	−19.03	−25.73
SW [a]	n.d.	n.d.	20.8	8.22	59	46,362	32,453	729.55	99.5	27.7	73.14	3.05	609.35	15.34	129.03	23.35	3.64	1.50 [b]	−6.77

[a] = from Cinti et al., 2011.
[b] Average $\delta^{13}C_{TDIC}$ value for seawater.

($\delta^{13}C_{CO2} = -1.55$‰ vs. VPDB, Barberi et al., 2007), located at about 1 km away from the site where gaseous eruption occurred in the 24th of August.

4. Discussion and conclusions

The Roman area and most part of the central–western Italy is characterized by high levels of deep CO_2 (and other minor gases) degassing (Minissale et al., 2002; Chiodini et al., 2004, 2008; Gambardella et al., 2004). In this area, where degassing is not manifested through, for instance, obvious hydrothermal springs or fumaroles, the apparent lack of degassing may be a symptom that CO_2 and other endogenous gases are substantially sealed in subsurface geological traps, from where they could suddenly escape in the case of human intervention (e.g., drilling or excavation; Barberi et al., 2007; Carapezza and Tarchini, 2007) or also by natural processes (e.g., faulting and fracturing, seismically-induced shaking and CO_2 exsolution; Manga and Brodsky, 2006; Uysal et al., 2007, 2009; De Filippis et al., 2013a). The case of gas shallow entrapment applies to the Fiumicino area, where manifestation of natural degassing is substantially absent or still poorly known (Chiodini et al., 2000, 2008), but episodes of gas blowouts induced by well drilling happened in 1925, 2005, 2013, and several other times (Novarese, 1926; Barberi et al., 2007; Carapezza et al., 2010; Pantaloni and Argentieri, 2013), thus demonstrating the subsurface widespread entrapment of gases. It is noteworthy that, in the 2005 case reported by Barberi et al. (2007), seven persons inhabiting in houses close to the CO_2 emitting well requested medical assistance and were hospitalized due to strong headache and other symptoms including also loss of consciousness (Barberi et al., 2007). It is therefore of paramount importance to understand how gases become entrapped in the Fiumicino area subsurface.

Our results, together with previous studies, show that CO_2 and other minor gases in the Fiumicino area are entrapped in the PGS mid-Pleistocene gravel horizon (5–10 m thick) lying at a depth of about 40–50 m between the Lower Pleistocene MDP silty clays and the Upper Pleistocene TDS organic rich silty clays (Figs. 3 and 4). The main evidence for this entrapment is constituted by the fluid high pressure recorded by one of us (P.S.) during borehole drilling in the Fiumicino area when approaching the gravel depth (S4 and S5 boreholes; Fig. 4). The aquifer hosted by the gravel horizon can act as a buffer for endogenous gases (e.g., Crossey et al., 2006, 2009), hampering the possible natural upraise of the free gas phase toward the surface throughout the overlying TDS Upper Pleistocene silty clays (Figs. 3 and 4). Carbon isotopes emphasized that the pressurized gas hosted in the gravel horizon is inorganic-derived (i.e., deep) CO_2, (Ciotoli et al., 2013) whereas unconfined aquifers dissolve a prevalent biogenic-derived (i.e., shallow) CO_2. The two layers are completely separated by the impermeable Upper Pleistocene silty clays, and the two hosted aquifers are hydraulically unconnected (Fig. 4). $\delta^{13}C$ of the deep CO_2 (Ciotoli et al., 2013) falls in the range of the values measured in the gas emissions located in the western sector of central Italy, suggesting that CO_2 could derive both from the mantle and thermo-metamorphism of carbonates, mixed at various extent. For this reason, we named as “fumarole” the fluid vent recently emerged at Fiumicino (i.e., fumarole: a volcanic vent, distinct from those erupting magma, from which volcanic gases escape). Moreover, geochemical data referred to the (deep) CO_2 emitted at the fumarole are fully comparable with those reported by previous studies conducted in the same area when similar degassing episodes occurred (Barberi et al., 2007; Carapezza and Tarchini, 2007). In particular, in the gases blown out during the drilling of a well located close to the Fiumicino fumarole (February 2005), Barberi et al. (2007) found mainly CO_2 (98 vol.%) accompanied by minor contents of N_2 and CH_4. The isotopic and chemical composition ($\delta^{13}C_{CO2} = -1.55$ and $^3He/^4He = 0.314$ Ra) of the emitted gases revealed an affinity with gas manifestations from the adjacent Sabatini and Colli Albani volcanic districts, particularly from the first district. These authors stated that the gases emitted in the 2005 case had a significant component originated in

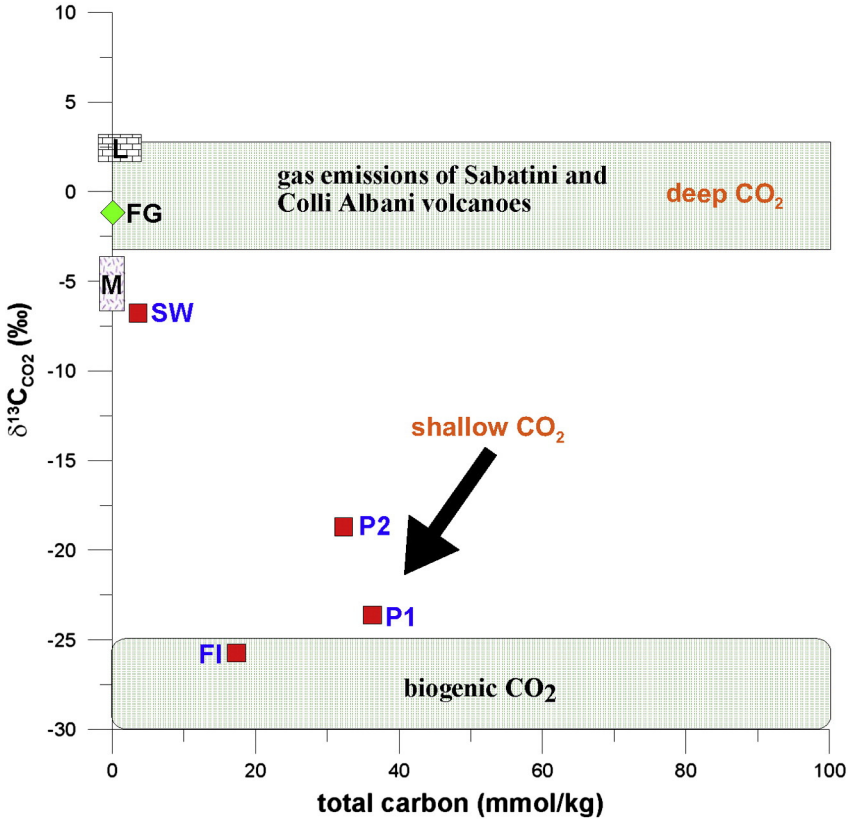

Fig. 8. Total carbon vs. calculated $\delta^{13}C_{CO2}$. Samples FI, P1, and P2 show largely negative $\delta^{13}C_{CO2}$ values, implying a dominant shallow-derived CO_2 (black arrow), while CO_2 emitted at fumarole (FG, Ciotoli et al., 2013) shows a carbon isotope signature (green diamond) pointing to a completely different origin of dissolved CO_2, probably due to both mantle degassing and thermo-metamorphic reactions involving carbonate formations. For comparison, are reported: (*i*) the range of the $\delta^{13}C_{CO2}$ values measured in the gas manifestations of both Colli Albani and Sabatini volcanoes; (*ii*) $\delta^{13}C_{CO2}$ range of biogenic-derived CO_2; (*iii*) $\delta^{13}C_{CO2}$ range of Apenninic limestones (L, Chiodini et al., 2004); and (*iv*) $\delta^{13}C_{CO2}$ range of mantle (M, Javoy et al., 1982; Rollinson, 1993). (For interpretation of the references to color in this figure, the reader is referred to the web version of this article.)

the mantle, which, beneath the Roman area, is probably deeply contaminated with crustal material, showing a ^{13}C enrichment as compared with the Italian high-temperature volcanic gases (Panichi and Tongiorgi, 1976; Minissale, 1991; Chiodini et al., 2000; Chiodini and Frondini, 2001; Minissale, 2004; Mariucci et al., 2008).

It is interesting to notice that the Fiumicino fumarole has kept degassing for weeks since 24 August, 2013, and it is still active at the time of writing (November 2013). This process implies that the gas reservoir is large and, perhaps, continuously fed (see also Novarese, 1926; Pantaloni and Argentieri, 2013). This evidence is consistent with our geophysical data that support a lateral continuity of the studied stratigraphic units (including the Middle Pleistocene gravel; Fig. 5) and with the fact that the gravel layer is intercepted by all boreholes in the Fiumicino area and also in the surrounding larger region (see borehole-data-based cross-sections in Bellotti et al., 1995; Bozzano et al., 2008; Funiciello and Giordano, 2008; Funiciello et al., 2008; Praturlon, 2008; Raspa et al., 2008; Marra et al., 2013; Milli et al., 2013). Moreover, degassing in the 1925 case lasted for about one year (Novarese, 1926). In other words, the gas reservoir is most probably not a local pocket of gravel, as also demonstrated by the fact that other phenomena of well gas blowout occurred in all the Fiumicino area including its offshore (see details below). The above-reported hypothesis of a continuously fed subsurface gas reservoir implies that this stored gas has to leak upward. Evident manifestations (diffuse or discrete) of degassing in the Fiumicino area are still substantially unreported in the scientific literature, although ongoing studies are starting to show a widespread and pervasive phenomenon of degassing in this area (e.g.,Tuccimei et al., 2007; Ciotoli et al., 2013).

Concerning the trigger, the Fiumicino fumarole emerged from a shallow (30 m of maximum depth) borehole drilled in the hours or days preceding the first emergence (e.g., Corriere.it, 2013; IlFaroonline.it, 2013; IlGiornaleDellaProtezioneCivile.it, 2013; Terzobinario.it, 2013). This borehole did not extend down to the CO_2-rich gravel layer (i.e., 40–50 m deep) and did not blow out for gas overpressure during drilling. The fumarole emerged soon after the drilling, probably for the drilling-related reduced sedimentary cover that restrained the CO_2-rich gravel layer. We can hence assert that the fumarole was artificially triggered.

In synthesis, we propose a model (Fig. 9) for gas entrapment at shallow levels in the Fiumicino area consisting of ascending endogenous gases (mainly CO_2). These gases can slowly permeate the Lower Pleistocene hard silty clays through fractures, thus reaching the permeable mid-Pleistocene gravel layer. Upward, the aquifer is confined by the impermeable Upper Pleistocene clays and silty clays and acts as a buffer against the ascending endogenous gases, thus resulting in a gas pressurized aquifer, which can constitute a source of hazard during excavation activities.

5. In conclusion

(1) Endogenous degassing in central–western Italy is very high (Gambardella et al., 2004; Chiodini et al., 2008). Where this phenomenon is apparently absent, such as in the Fiumicino area (Tiber River delta), CO_2 and other endogenous gases may be entrapped in shallow levels as demonstrated in this paper and in previous ones (e.g., Novarese, 1926; Barberi et al., 2007; Carapezza and Tarchini, 2007), thus constituting a potential source of hazard. We point out the importance of both stratigraphic setting (i.e. the presence of a thick shallow impermeable clay layer) and the presence of an aquifer in the gravel horizon

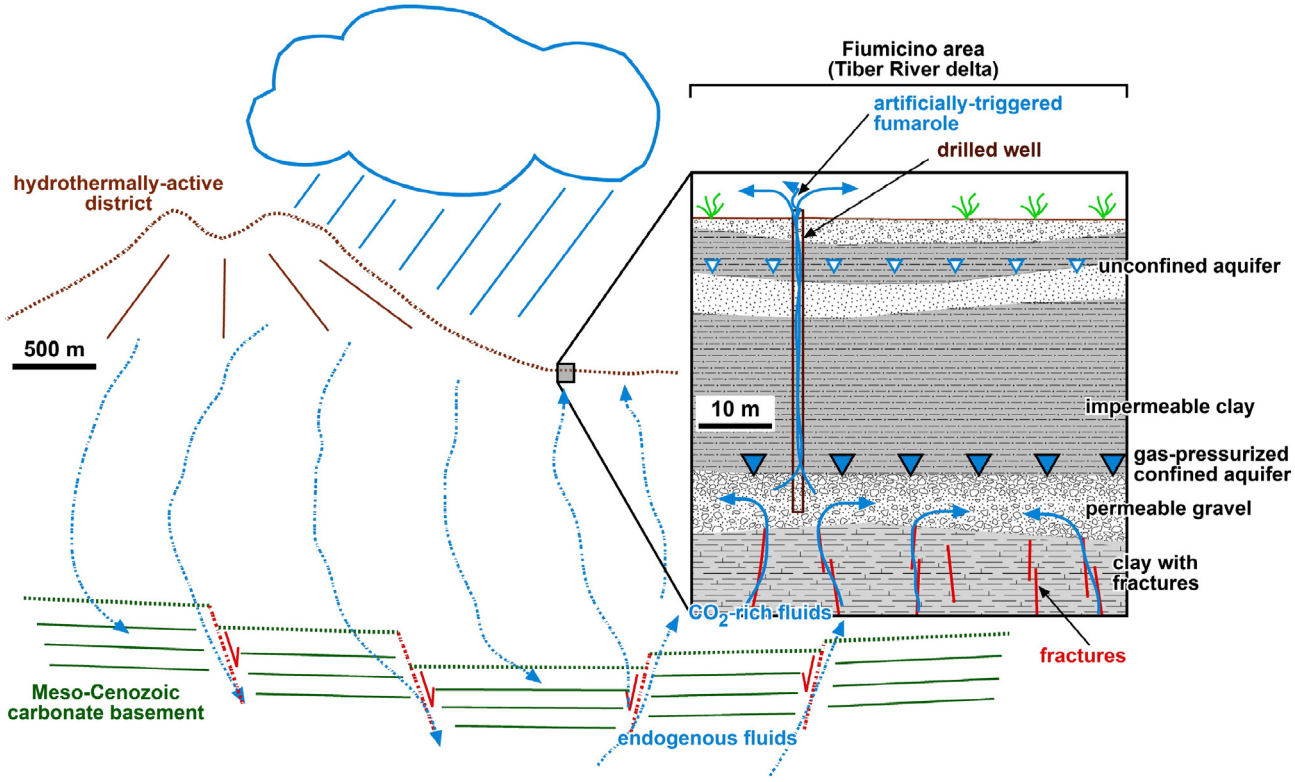

Fig. 9. Conceptual model of fluid circulation in the Fiumicino subsurface (compare it with Figs. 3 and 4) within a hypothetical broader context of fluid circulation. Ascending endogenous fluids (mantle fluids mixed with a crustal component derived from thermal decarbonation of deep carbonates) pass through the basal Lower Pleistocene clays thanks to the presence of some fractures and are upward buffered by the confined aquifer residing in the mid-Pleistocene gravel. The aquifer becomes gas-pressurized thus constituting a potential source of hazard in the case of drilling or other types of excavations.

acting as a buffer for CO_2 upraise, to minimize the possibility of degassing in "undisturbed" (i.e. natural) conditions;

(2) As the stratigraphy of the Fiumicino area is very common in large portions of the densely-populated Roman area and as the adjacent volcanic districts are hydrothermally active, sudden degassing phenomena similar to the one recently observed at Fiumicino could again occur at Fiumicino and elsewhere in the surrounding region, mainly if artificially triggered (e.g., Novarese, 1926; Pantaloni and Argentieri, 2013);

(3) Any drilling or other types of excavations in the Fiumicino area and not only are thus exposed to hazards from gas sudden blow-outs. Preventive geological-stratigraphic studies and precautionary operative measures should therefore be undertaken when operating excavations and similar activities;

(4) As a timely confirmation of our previous conclusions, we signal that, on 26 September 2013, while writing this paper, further sudden degassing phenomena occurred a few tens of meters off the Tiber River delta (off Fiumicino) as a consequence of excavation activities (borehole drilling) connected with the construction of the new Fiumicino harbor (Supplemental Materials 4 and 5).

Acknowledgments

We thank the Fiumicino Municipality for financing the stratigraphic and geophysical campaigns carried out by Geomagellan (P. Sella). A.B. thanks G. Ciotoli, M. Lustrino, and F. Trippetta for fruitful discussions. We also thank D. Cinti for carrying out chemical analyses of the Fiumicino groundwater. We acknowledge the invaluable work of historical research by A. Argentieri and M. Pantaloni (http://www.geoitaliani.it), who have rightly brought to our attention the degassing events, which occurred at Fiumicino in 1925. We thank A. Brogi and L. Crossey for their constructive reviews, and the Editor, M. Mangan, and her staff for the careful editorial work.

Appendix A. Supplementary data

Supplementary data associated with this article can be found in the online version, at http://dx.doi.org/10.1016/j.jvolgeores.2014.05.008. These data include Google maps of the most important areas described in this article.

References

Acocella, V., Funiciello, R., 2006. Transverse systems along the extensional Tyrrhenian margin of central Italy and their influence on volcanism. Tectonics 25, TC2003. http://dx.doi.org/10.1029/2005TC001845.

Alvarez, W., Ammerman, A.J., Renne, P.R., Karner, D.B., Terrenato, N., Montanari, A., 1996. Quaternary fluvial–volcanic stratigraphy and geochronology of the Capitoline Hill in Rome. Geology 24, 751–754.

Annunziatellis, A., Ciotoli, G., Lombardi, S., Nolasco, F., 2003. Short- and long-term gas hazard: the release of toxic gases in the Alban Hills volcanic area (central Italy). J. Geochem. Explor. 77, 93–108.

Argentieri, A., Pantaloni, M., 2013. Novarese, Vittorio. Dizionario Biografico degli Italiani. Istituto dell'Enciclopedia Italiana fondata da Giovanni Treccani, Roma (available online at http://www.treccani.it/enciclopedia/vittorio-novarese_(Dizionario-Biografico)/).

Bais, G., Bruno, P.G., Di Fiore, V., Rapolla, A., 2003. Characterization of shallow volcanoclastic deposits by turning ray seismic tomography: an application to the Naples urban area. J. Appl. Geophys. 52, 11–21.

Barberi, F., Carapezza, M.L., Ranaldi, M., Tarchini, L., 2007. Gas blowout from shallow boreholes at Fiumicino (Rome): induced hazard and evidence of deep CO_2 degassing on the Tyrrhenian margin of Central Italy. J. Volcanol. Geotherm. Res. 165, 17–31.

Barbieri, M., Masi, U., Tolomeo, L., 1979. Origin and distribution of strontium in the travertines of Latium (central Italy). Chem. Geol. 24, 181–188.

Barchi, M., 2010. The Neogene–Quaternary evolution of the Northern Apennines: crustal structure, style of deformation and seismicity. J. Virtual Explor. 36, 11. http://dx.doi.org/10.3809/jvirtex.2010.00220.

Barrocu, G., 2003. Seawater Intrusion in the Coastal Aquifers of Italy. In: Calaferra, J. (Ed.), State of Seawater Intrusion in Coastal Aquifers of the Mediterranean Coast, Alicante, pp. 207–223.

Beaubien, S.E., Ciotoli, G., Lombardi, S., 2003. Carbon dioxide and radon gas hazard in the Alban Hills area (Central Italy). J. Volcanol. Geotherm. Res. 123, 63–80.
Bellotti, P., Milli, S., Tortora, P., Valeri, P., 1995. Physical stratigraphy and sedimentology of the Late Pleistocene–Holocene Tiber Delta depositional sequence. Sedimentology 42, 617–634.
Billi, A., Tiberti, M.M., 2009. Possible causes of arc development in the Apennines, central Italy. Geol. Soc. Am. Bull. 121, 1409–1420.
Billi, A., Tiberti, M.M., Cavinato, G.P., Cosentino, D., Di Luzio, E., Keller, J.V.A., Kluth, C., Orlando, L., Parotto, M., Praturlon, A., Romanelli, M., Storti, F., Wardell, N., 2006. First results from the CROP-11 deep seismic profile, central Apennines, Italy: evidence of mid-crustal folding. J. Geol. Soc. Lond. 163, 583–586.
Billi, A., Valle, A., Brilli, M., Faccenna, C., Funiciello, R., 2007. Fracture-controlled fluid circulation and dissolutional weathering in sinkhole-prone carbonate rocks from central Italy. J. Struct. Geol. 29, 385–395.
Bordoni, P., Valensise, G., 1998. Deformation of the 125 ka Marine Terrace in Italy: Tectonic Implications. In: Stewart, I.S., Vita-Finzi, C. (Eds.), Coastal Tectonics. Geological Society London, Special Publication, 146, pp. 71–110.
Bozzano, F., Caserta, A., Govoni, A., Marra, F., Martino, S., 2008. Static and dynamic characterization of alluvial deposits in the Tiber River Valley: new data for assessing potential ground motion in the City of Rome. J. Geophys. Res. 113, B01303. http://dx.doi.org/10.1029/2006JB004873.
Brogi, A., 2011. Bowl-shaped basin related to low-angle detachment during continental extension: the case of the controversial Neogene Siena Basin (central Italy, Northern Apennines). Tectonophysics 499, 54–76.
Brogi, A., Capezzuoli, E., 2009. Travertine deposition and faulting: the fault-related travertine fissure-ridge at Terme S. Giovanni, Rapolano Terme (Italy). Int. J. Earth Sci. (Geol. Rundsch.) 98, 931–947.
Brogi, A., Liotta, D., 2008. Highly extended terrains, lateral segmentation of the substratum, and basin development: the middle–late Miocene Radicondoli Basin (inner northern Apennines, Italy). Tectonics 27, TC5002. http://dx.doi.org/10.1029/2007TC002188.
Brogi, A., Liotta, D., Meccheri, M., Fabbrini, L., 2010. Transtensional shear zones controlling volcanic eruptions: the Middle Pleistocene Mt Amiata volcano (inner Northern Apennines, Italy). Terra Nova 22, 137–146.
Caliro, S., Chiodini, G., Moretti, R., Avino, R., Granieri, D., Russo, M., Fiebig, J., 2007. The origin of the fumaroles of La Solfatara (Campi Flegrei, South Italy). Geochim. Cosmochim. Acta 71, 3040–3055.
Capelli, G., Mazza, R., 2008. Intrusione salina nel delta del Fiume Tevere. Evoluzione del fenomeno nei primi anni del terzo millennio (in Italian). In: Funiciello, R., Praturlon, A., Giordano, G. (Eds.), Mem. Descr. della Carta Geol. d'It, vol. 80.
Capelli, G., Mazza, R., Taviani, S., 2008. Acque sotterranee nella città di Roma (in Italian). In: Funiciello, R., Praturlon, A., Giordano, G. (Eds.), Mem. Descr. della Carta Geol. d'It, vol. 80.
Carapezza, M.L., Tarchini, L., 2007. Accidental gas emission from shallow pressurized aquifers at Alban Hills volcano (Rome, Italy): geochemical evidence of magmatic degassing? J. Volcanol. Geotherm. Res. 165, 5–16.
Carapezza, M.L., Barberi, F., Tarchini, L., Ranaldi, M., Ricci, T., 2010. Volcanic hazards of the Colli Albani. Special Publications of IAVCEI, 3. Geological Society, London pp. 279–297.
Carapezza, M.L., Barberi, F., Ranaldi, M., Ricci, T., Tarchini, L., Barrancos, J., Fischer, C., Granieri, D., Lucchetti, C., Melian, G., Perez, N., Tuccimei, P., Vogel, A., Weber, K., 2012. Hazardous gas emissions from the flanks of the quiescent Colli Albani volcano (Rome, Italy). Appl. Geochem. 27, 1767–1782.
Cavinato, G., DeCelles, P.G., 1999. Extensional basins in tectonically bimodal central Apennines fold-thrust belt, Italy: response to corner flow above a subducting slab in retrograde motion. Geology 27, 955–958.
Cerling, T.E., Solomon, D.K., Quade, J., Bowman, J.R., 1991. On isotopic composition of carbon in soil carbon dioxide. Geochim. Cosmochim. Acta 55, 3403–3405.
Chiodini, G., Frondini, F., 2001. Carbon dioxide degassing from the Albani Hills volcanic region, Central Italy. Chem. Geol. 177, 67–83.
Chiodini, G., Frondini, F., Cardellini, C., Parello, F., Peruzzi, L., 2000. Rate of diffuse carbon dioxide Earth degassing estimated from carbon balance of regional aquifers: the case of Central Apennine, Italy. J. Geophys. Res. 105, 8423–8434.
Chiodini, G., Cardellini, C., Amato, A., Boschi, E., Caliro, S., Frondini, F., 2004. Carbon dioxide Earth degassing and seismogenesis in Central and southern Italy. Geophys. Res. Lett. 31, L07615. http://dx.doi.org/10.1029/2004GL019480.
Chiodini, G., Valenza, M., Cardellini, C., Frigeri, A., 2008. A new web-based catalog of Earth degassing sites in Italy. EOS Trans. Am. Geophys. Union 89, 341–342. http://dx.doi.org/10.1029/2008EO370001.
Chiodini, G., Caliro, S., Lowenstern, J.B., Evans, W.C., Bergfeld, D., Tassi, F., Tedesco, D., 2012. Insights from fumarole gas geochemistry on the origin of hydrothermal fluids on the Yellowstone Plateau. Geochim. Cosmochim. Acta 89, 265–278.
Cinti, D., Procesi, M., Tassi, F., Montegrossi, G., Sciarra, A., Vaselli, O., Quattrocchi, F., 2011. Fluid geochemistry and geothermometry in the western sector of the Sabatini Volcanic District and the Tolfa Mountains (Central Italy). Chem. Geol. 284 (1–2), 160–181.
Cioni, R., Laurenzi, M.A., Sbrana, A., Villa, I.M., 1993. 40Ar/39Ar chronostratigraphy of the initial activity in the Sabatini Volcanic Complex (Italy). Boll. Soc. Geol. Ital. 112, 251–263.
Ciotoli, G., Etiope, G., Florindo, F., Marra, F., Ruggiero, L., Sauer, P.E., 2013. Sudden deep gas eruption nearby Rome's airport of Fiumicino. Geophys. Res. Lett. http://dx.doi.org/10.1002/2013GL058132.
Corriere.it, 2013. Fiumicino, nuovo geyser ma in mare è la terza bocca del mini-vulcano. Available online at http://roma.corriere.it/roma/notizie/cronaca/13_settembre_27/fiumicino-mini-vulcano-tris-ispezione%20-2223325491942.shtml.
Crossey, L.J., Fischer, T.P., Patchett, P.J., Karlstrom, K.E., Hilton, D.R., Newell, D.L., Huntoon, P., Reynolds, A.C., de Leeuw, G.A.M., 2006. Dissected hydrologic system at the Grand Canyon: interaction between deeply derived fluids and plateau aquifer waters in modern springs and travertine. Geology 34, 25–28.
Crossey, L.J., Karlstrom, K.E., Springer, A.E., Newell, D., Hilton, D.R., Fischer, T., 2009. Degassing of mantle-derived CO_2 and He from springs in the southern Colorado Plateau region — neotectonic connections and implications for groundwater systems. Geol. Soc. Am. Bull. 121, 1034–1053.
De Benedetti, A.A., Funiciello, R., Giordano, G., Diano, G., Caprilli, E., Paterne, M., 2008. Volcanology, history and myths of the Lake Albano maar (Colli Albani volcano, Italy). J. Volcanol. Geotherm. Res. 176, 387–406.
De Filippis, L., Anzalone, E., Billi, A., Faccenna, C., Poncia, P.P., Sella, P., 2013a. The origin and growth of a recently-active fissure ridge travertine over a seismic fault, Tivoli, Italy. Geomorphology 195, 13–26.
De Filippis, L., Faccenna, C., Billi, A., Anzalone, E., Brilli, M., Soligo, M., Tuccimei, P., 2013b. Plateau versus fissure ridge travertines from Quaternary geothermal springs of Italy and Turkey: interactions and feedbacks among fluid discharge, paleoclimate, and tectonics. Earth Sci. Rev. 123, 35–52.
De Luca, A., Preziosi, E., Giuliano, G., Mastroianni, D., Falconi, F., 2004. First evaluation of the saltwater intrusion in the Tiber delta area (Rome, central Italy). 18th SWIM, Cartagena, Spain.
De Rita, D., Funiciello, R., Parotto, M., 1988. Carta Geologica del Complesso Vulcanico dei Colli Albani (scale 1: 50.000). Progetto Finalizzato Geodinamica, Consiglio Nazionale delle Ricerche, Roma.
De Rita, D., Funiciello, R., Corda, L., Sposato, A., Rossi, U., 1993. Volcanic Unit. In: Di Filippo, M. (Ed.), Sabatini Volcanic Complex. Progetto Finalizzato " Geodinamica" Monografie Finali, 11. Consiglio Nazionale Delle Ricerche, pp. 33–79.
De Rita, D., Faccenna, C., Funiciello, R., Rosa, C., 1995. Stratigraphy and volcano-tectonics. In: Trigila, R. (Ed.), The Volcano of the Alban Hills. Tipografia S.G.S., Rome, pp. 33–71.
De Rita, D., Di Filippo, M., Rosa, C., 1996. Structural Evolution of the Bracciano Volcano-Tectonic Depression, Sabatini Volcanic District, Italy. In: McGuire, W.J., Jones, A.P., Neuberg, J. (Eds.), Volcano Instability on the Earth and Other Planets. Geological Society Special Publication, 110, pp. 225–236.
Dèzes, P., Ziegler, P.A., 2002. Moho depth map of Western and Central Europe. World Wide Web Address http://comp1.geol.unibas.ch/downloads/Moho_net/euromoho1_3.pdf.
Di Filippo, M., Toro, B., 1995. Gravity features. In: Trigila, R. (Ed.), The Volcano of the Alban Hills. Tipografia SGS, Roma, pp. 213–219.
Etiope, G., Fridriksson, T., Italiano, F., Winiwarter, W., Theloke, J., 2007. Natural emissions of methane from geothermal and volcanic sources in Europe. J. Volcanol. Geotherm. Res. 165, 76–86.
Faccenna, C., Funiciello, R., Bruni, A., Mattei, M., Sagnotti, L., 1994a. Evolution of a transfer-related basin: the Ardea basin (Latium, central Italy). Basin Res. 6, 35–46.
Faccenna, C., Funiciello, R., Montone, P., Parotto, M., Voltaggio, M., 1994b. Late Pleistocene strike-slip tectonics in the Acque Albule Basin (Tivoli, Latium). Memorie Descrittive della Carta Geologica d'Italia, 49 pp. 37–50.
Faccenna, C., Soligo, M., Billi, A., De Filippis, L., Funiciello, R., Rossetti, C., Tuccimei, P., 2008. Late Pleistocene depositional cycles of the Lapis Tiburtinus travertine (Tivoli, Central Italy): possible influence of climate and fault activity. Glob. Planet. Chang. 63, 299–308.
Funiciello, R. (Ed.), 1995. La Geologia di Roma. Il Centro Storico. Memorie Descrittive della carta Geologica d'Italia, 50, p. 550.
Funiciello, R., Giordano, G. (Eds.), 2008. Note illustrative della Carta Geologica d'Italia alla scala 1:50.000, foglio 374 Roma. Agenzia per la Protezione dell'Ambiente e per i Servizi Tecnici, Rome, pp. 158.
Funiciello, R., Giordano, G. (Eds.), 2010. The Colli Albani Volcano. Special Publication of IAVCEI, 3. The Geological Society of London, London, p. 400.
Funiciello, R., Parotto, M., 1978. Il substrato sedimentario nell'area dei Colli Albani: considerazioni geodinamiche e paleogeografiche sul margine tirrenico dell'Appennino centrale. Geologica Romana, 17 pp. 233–287.
Funiciello, R., Locardi, E., Parotto, M., 1976. Lineamenti geologici dell'area sabatina orientale. Boll. Soc. Geol. Ital. 95, 831–849.
Funiciello, R., Giordano, G., De Rita, D., Carapezza, M.L., Barberi, F., 2002. L'attività recente del Lago Albano di Castelgandolfo. Rendiconti Lincei, 9 pp. 113–143.
Funiciello, R., Giordano, G., De Rita, D., 2003. The Albano maar lake (Colli Albani Volcano, Italy): recent volcanic activity and evidence of pre-Roman Age catastrophic lahar events. J. Volcanol. Geotherm. Res. 123, 43–61.
Funiciello, R., Praturlon, A., Giordano, G. (Eds.), 2008. La Geologia di Roma. Dal centro Storico alla Periferia. Il Centro Storico. Memorie Descrittive della carta Geologica d'Italia, 80, p. 765.
Gambardella, B., Cardellini, C., Chiodini, G., Frondini, F., Marini, L., Ottonello, G., Vetuschi Zoccolino, M., 2004. Fluxes of deep CO_2 in the volcanic areas of central–southern Italy. J. Volcanol. Geotherm. Res. 136, 31–52.
Giaccio, B., Sposato, A., Gaeta, M., Marra, F., Palladino, D.M., Taddeucci, J., Barbieri, M., Messina, P., Rolfo, M.F., 2007. Mid-distal occurrences of the Albano maar pyroclastic deposits and their relevance for reassessing the eruptive scenarios of the most recent activity at the Colli Albani Volcanic District, Central Italy. Quat. Int. 171–172, 160–178.
Giammanco, S., Parello, F., Gambardella, B., Schifano, R., Pizzullo, S., Galante, G., 2007. Focused and diffuse effluxes of CO_2 from mud volcanoes and mofettes south of Mt. Etna (Italy). J. Volcanol. Geotherm. Res. 165, 46–63.
Gioia, P., Harnoldus-Huyzendveld, A., Celant, A., Rosa, C., Volpe, R., 2010. Archaeological Investigations in the Torre Spaccata valley (Rome): Human Interaction with the Recent Activity of the Albano Maar. In: Funiciello, R., Giordano, G. (Eds.), The Colli Albani Volcano. Special Publication of IAVCEI, 3. The Geological Society, London, pp. 355–382.
Giordano, G., Mazza, R., 2010. The Geology of Rome and Urban Areas: The Legacy of Prof. Renato Funiciello. In: Beltrando, Marco, Peccerillo, Angelo, Mattei, Massimo, Conticelli, Sandro, Doglioni, Carlo (Eds.), The Geology of Italy: tectonics and life

along plate margins. Journal of the Virtual Explorer. 1441-8142, vol. 36, paper 28. 28. http://dx.doi.org/10.3809/jvirtex.2010.00277 (Electronic Edition).
Giordano, G., De Rita, D., Fabbri, M., Rodani, S., 2002. Facies associations of rain generated versus crater lake-withdrawal lahar deposits from Quaternary volcanoes, central Italy. J. Volcanol. Geotherm. Res. 118, 145–159.
Giordano, G., Esposito, A., De Rita, D., Fabbri, M., Mazzini, I., Trigari, A., Rosa, C., Funiciello, R., 2003. The sedimentation along the Roman coast between middle and upper Pleistocene: the interplay of eustatism, tectonics and volcanism — new data and review. Il Quaternario, 16 pp. 121–129 (1Bis).
Giordano, G., De Benedetti, A.A., Diana, A., Diano, G., Gaudioso, F., Marasco, F., Miceli, M., Mollo, S., Cas, R.A.F., Funiciello, R., 2006. The Colli Albani mafic caldera (Roma, Italy): stratigraphy, structure and petrology. J. Volcanol. Geotherm. Res. 155, 49–80.
Giordano, G., De Benedetti, A.A., Bonamico, A., Ramazzotti, P., Mattei, M., 2013. Incorporating surface indicators of reservoir permeability into reservoir volume calculations: application to the Colli Albani caldera and the Central Italy Geothermal Province. Earth Sci. Rev. http://dx.doi.org/10.1016/j.earscirev.2013.10.010.
Hannington, M., Herzig, P., Stoffers, P., Scholten, J., Botz, R., Garbe-Schönberg, D., Jonasson, I.R., Roest, W., Shipboard Scientific Party, 2001. First observations of high-temperature submarine hydrothermal vents and massive anhydrite deposits off the north coast of Iceland. Mar. Geol. 177, 199–220.
Heincke, B., Günther, T., Dalsegg, E., Rønning, J.S., Ganerød, G.V., Elvebakk, H., 2010. Combined three-dimensional electric and seismic tomography study on the Åknes rockslide in western Norway. J. Appl. Geophys. 70, 292–306.
IlFaroonline.it, 2013. Montino: "Geyser a Coccia di Morto, le perforazioni erano di Italgas". Available online at http://www.ilfaroonline.it/2013/08/27/fiumicino/montino-geyser-a-coccia-di-morto-le-perforazioni-erano-di-italgas-39284.html.
IlGiornaleDellaProtezioneCivile.it, 2013. Fiumicino: un vulcanetto di fango spunta in città. Available online at http://www.ilgiornaledellaprotezionecivile.it/?pg=1&idart=10092&idcat=3.
Javoy, M., Pineau, F., Allegre, C.J., 1982. Carbon geodynamic cycle. Nature 300, 171–173.
Karner, D.B., Marra, F., Renne, P.R., 2001. The history of the Monti Sabatini and Alban Hills volcanoes: groundwork for assessing volcanic-tectonic hazards for Rome. J. Volcanol. Geotherm. Res. 107, 185–219.
Kopf, A.J., 2002. Significance of mud volcanism. Rev. Geophys. 40, 1–52.
Locardi, E., Lombardi, G., Funiciello, R., Parotto, M., 1976. The main volcanic group of Lazio (Italy): relations between structural evolution and petrogenesis. Geol. Romana 15, 279–300.
Maiorani, A., Funiciello, R., Mattei, M., Turi, B., 1992. Stable isotope geochemistry and structural elements of the Sabina region (Central Apennines, Italy). Terra Nova 4, 484–488.
Malinverno, A., Ryan, W., 1986. Extension in the Tyrrhenian Sea and shortening in the Apennines as result of arc migration driven by sinking of the lithosphere. Tectonics 5, 227–245.
Manga, M., Brodsky, E., 2006. Seismic triggering of eruptions in the far field: volcanoes and geysers. Annu. Rev. Earth Planet. Sci. 34, 263–291.
Mariucci, M.T., Pierdominici, S., Pizzino, L., Marra, F., Montone, P., 2008. Looking into a volcanic area: an overview on the 350 m scientific drilling at Colli Albani (Rome, Italy). J. Volcanol. Geotherm. Res. 176, 225–240.
Marra, F., Karner, D.B., Freda, C., Gaeta, M., Renne, P., 2009. Large mafic eruptions (central Italy): chronostratigraphy, petrography and eruptive behavior. J. Volcanol. Geotherm. Res. 179, 217–232.
Marra, F., Bozzano, F., Cinti, F.R., 2013. Chronostratigraphic and lithologic features of the Tiber River sediments (Rome, Italy): implications on the post-glacial sea-level rise and Holocene climate. Glob. Planet. Chang. 107, 157–176.
Mazzini, A., 2009. Mud volcanism: processes and implications. Mar. Pet. Geol. 26, 1677–1680.
McCrea, J., 1950. On the isotopic chemistry of carbonates and a paleotemperature scale. J. Chem. Phys. 18, 849–857.
Milli, S., 1997. Depositional setting and high-frequency sequence stratigraphy of the middle–upper Pleistocene to Holocene deposits of the Roman basin. Geol. Romana 33, 99–136.
Milli, S., D'Ambrogi, C., Bellotti, P., Calderoni, G., Carboni, M.G., Celant, A., Di Bella, L., Di Rita, F., Frezza, V., Magri, D., Pichezzi, M.R., Ricci, V., 2013. The transition from wave-dominated estuary to wave-dominated delta: the Late Quaternary stratigraphic architecture of Tiber River deltaic succession (Italy). Sediment. Geol. 284–285, 159–180.
Minissale, A., 1991. Thermal springs in Italy: their relation to recent tectonics. Appl. Geochem. 6, 201–212.
Minissale, A., 2004. Origin, transport and discharge of CO2 in central Italy. Earth Sci. Rev. 66, 89–141.
Minissale, A., Evans, W.C., Magro, G., Vaselli, O., 1997. Multiple source components in gas manifestations from north–central Italy. Chem. Geol. 142, 175–192.
Minissale, A., Kerrick, D.M., Magro, G., Murrell, M.T., Paladini, M., Rihs, S., Sturchio, N.C., Tassi, F., Vaselli, O., 2002. Geochemistry of Quaternary travertines in the region north of Rome (Italy): structural, hydrologic, and paleoclimatic implications. Earth Planet. Sci. Lett. 203, 709–728.
Mongelli, F., Zito, G., 1991. Flusso di calore nella regione Toscana. Studi Geologici Camerti, special vol. 1991/1 pp. 91–98.
Novarese, V., 1926. La trivellazione di Fiumicino e le emanazioni di CO_2 del Vulcano laziale. Bollettino del Regio Ufficio geologico d'Italia, 51 pp. 1–9.
Ohba, T., Taniguchi, H., Miyamoto, T., Hayashi, S., Hasenaka, T., 2007. Mud plumbing system of an isolated phreatic eruption at Akita Yakeyama volcano, northern Honshu, Japan. J. Volcanol. Geotherm. Res. 161, 35–46.
Panichi, C., Tongiorgi, E., 1976. Carbon isotopic composition of CO_2 from springs, fumaroles, mofettes, and travertines of central and southern Italy: a preliminary prospection method of geothermal areas. Proc. 2nd U.N. Symp. Development and Use of Geothermal Energy, San Francisco, 20–29 May 1975, pp. 815–825.
Pantaloni, M., Argentieri, A., 2013. 1925: l'eruzione di Fiumicino. Geoitaliani. available online at http://www.geoitaliani.it/2013/10/1925-leruzione-di-fiumicino.html?spref=fb.
Parkhurst, D.L., Appelo, A.A.J., 1999. User's guide to PHREEQC (version 2) — a computer program for speciation, batch-reaction, one-dimensional transport and inverse geochemical modeling. U.S.G.S. Water Res. Inv. Rep. 99-4259 p. 312.
Patrick, M., Dean, K., Dehn, J., 2004. Active mud volcanism observed with Landsat 7 ETM+. J. Volcanol. Geotherm. Res. 131, 307–320.
Peccerillo, A., 1985. Roman Comagmatic Province (Central Italy): evidence for subduction-related magma genesis. Geology 13, 103–106.
Pizzino, L., Galli, G., Mancini, C., Quattrocchi, F.M., Scarlato, P., 2002. Natural gas hazard (CO_2, ^{222}Rn) within a quiescent volcanic region and its relations with tectonics: the case of the Ciampino-Marino area, Alban Hills volcano, Italy. Nat. Hazards 27, 257–282.
Praturlon, A., 2008. The old and the recent Tiber Delta (Fiumicino and Ostia, the beach and harbour of Rome). Memorie Descrittive della carta Geologica d'Italia, 80 pp. 221–235.
Quattrocchi, F., Calcara, M., 1998. Test-sites for earthquake prediction experiments within the Colli Albani region. Phys. Chem. Earth 23, 915–920.
Quattrocchi, F., Cantucci, B., Cinti, D., Galli, G., Pizzino, L., Sciarra, A., Voltattorni, N., 2013. Continuous/discrete geochemical monitoring of CO_2 natural analogues and of diffuse degassing structures (DDS): hints for CO_2 storage sites geochemical monitoring protocol. Energy Procedia 1, 2135–2142.
Raspa, G., Moscatelli, M., Stigliano, F., Patera, A., Marconi, F., Folle, D., Vallone, R., Mancini, M., Cavinato, G.P., Milli, S., Coimbra Leite Costa, J.F., 2008. Geotechnical characterization of the upper Pleistocene–Holocene alluvial deposits of Roma (Italy) by means of multivariate geostatistics: cross-validation results. Eng. Geol. 101, 251–268.
Rollinson, H., 1993. Using Geochemical Data. Longman Group, London.
Sartori, R., ODP LEG 107 Scientific Staff, 1989. Tentative basin evolution compared to deformations in the surrounding chains. In: Boriani, A., Bonafede, M., Piccardo, G.B., Vai, G.B. (Eds.), The Lithosphere in Italy. Accademia Nazionale dei Lincei, Rome, pp. 139–156.
Sottili, G., Palladino, D.M., Marra, F., Jicha, B., Karner, D.B., Renne, P., 2010. Geochronology of the most recent activity in the Sabatini Volcanic District, Roman Province, central Italy. J. Volcanol. Geotherm. Res. 196, 20–30.
Sottili, G., Palladino, D.M., Gaeta, M., Masotta, M., 2012. Origins and energetics of maar volcanoes: examples from the ultrapotassic Sabatini Volcanic District (Roman Province, Central Italy). Bull. Volcanol. 74, 163–186.
Terzobinario.it, 2013. Geyser ed emergenza CO2 a Fiumicino: E' ancora il caso di realizzare fossa traianea?. Available online at http://www.terzobinario.it/geyser-ed-emergenza-co2-a-fiumicino-e-ancora-il-caso-di-realizzare-fossa-traianea/21929.
Tuccimei, P., Giordano, G., Tedeschi, M., 2006. CO_2 release variations during the last 2000 years at the Colli Albani volcano (Roma, Italy) from speleothems studies. Earth Planet. Sci. Lett. 243, 449–462.
Tuccimei, P., Soligo, M., Arnoldus-Huyzendveld, A., Morelli, C., Carbonara, A., Tedeschi, M., Giordano, G., 2007. Datazioni U/Th di depositi carbonatici intercalati ai resti della via Portuense antica (Ponte galeria, Roma): attribuzione storico-archeologica della strada e documentazione cronologica dell'attività idrotermale del fondovalle tiberino. The Journal of Fasti Online 97, 1–9.
Uysal, I.T., Feng, Y., Zhao, J.X., Altunel, E., Weatherley, D., Karabacak, V., Cengiz, O., Golding, S.D., Lawrence, M.G., Collerson, K.D., 2007. U-series dating and geochemical tracing of late Quaternary travertine in co-seismic fissures. Earth Planet. Sci. Lett. 257 (3–4), 450–462.
Uysal, I.T., Feng, Y., Zhao, J.X., Isik, V., Nuriel, P., Golding, S.D., 2009. Hydrothermal CO_2 degassing in seismically active zones during the late Quaternary. Chem. Geol. 265, 442–454.
Voltaggio, M., Spadoni, M., 2007. Mapping of H_2S fluxes from the ground using copper passive samplers: an application study at the Zolforata di Pomezia degassing area (Alban Hills, Central Italy). J. Volcanol. Geotherm. Res. 179, 56–68.
Werner, C., Brantley, S.L., Boomer, K., 2000. CO_2 emissions related to the Yellowstone volcanic system 2. Statistical sampling, total degassing, and transport mechanisms. J. Geophys. Res. 105, 10,831–10,846.
Zhang, J., Quay, P.D., Wilbur, D.O., 1995. Carbon isotope fractionation during gas–water exchange and dissolution of CO2. Geochim. Cosmochim. Acta 82, 161–173.